

Received May 17, 2021; reviewed; accepted July 5, 2021

## Enhancing flotation of smithsonite by using 1,3,5-Triazinane-2,4,6-trithione as sulfidation

Kunzhong He <sup>1</sup>, Hepeng Zhou <sup>1</sup>, Yongbing Zhang <sup>1</sup>, Xuekun Tang <sup>1,2</sup>, Xianping Luo <sup>1,2</sup>, Haisheng Han <sup>3</sup>

<sup>1</sup> Faculty of Resource and Environmental Engineering, Jiangxi University of Science and Technology, Ganzhou 341000, China

<sup>2</sup> Jiangxi Key Laboratory of Mining & Metallurgy Environmental Pollution Control, Jiangxi University of Science and Technology, Ganzhou 341000, China

<sup>3</sup> School of Minerals Processing and Bioengineering, Central South University, Changsha 410083, China

Corresponding author: [luoxianping9491@163.com](mailto:luoxianping9491@163.com) (Xianping Luo)

**Abstract:** 1,3,5-Triazinane-2,4,6-trithione (TMT) was used for the first time as a sulfidation agent in the flotation of smithsonite. Results showed that 80.5% recovery rate could be obtained in the presence of TMT ( $5 \times 10^{-5}$  mol/L) and butyl xanthate ( $5 \times 10^{-4}$  mol/L). However, the recovery rate was only 59.4% when sodium sulfide ( $5 \times 10^{-5}$  mol/L) was used. Micro-flotation test and contact angle measurement showed that TMT activation was better than sodium sulfide activation. Besides, the contact angle increased from 32.44° (untreated) to 89.58° (treated with TMT), which was significantly higher than 50.2° (treated with sodium sulfide). Fourier Transform Infrared spectroscopy (FT-IR) and Zeta potential test showed the chemisorption of TMT on the smithsonite surface. The results of ICP spectral detection and solution chemistry calculation revealed that Zn<sub>3</sub>TMT complex precipitates in the smithsonite pulp were formed on the mineral surface at pH 6.5. A hydrophobic film was also formed on the mineral surface after TMT treatment, and more adsorption sites were provided for butyl xanthate. Thus, the adsorption of collector was significantly enhanced.

**Keywords:** smithsonite, 1,3,5-Triazinane-2,4,6-trithione (TMT), sodium sulfide, flotation, sulfidation

### 1. Introduction

Zinc is widely used in the fields of machinery, metallurgy, electricity, military industry, chemistry, medicine, and light industry due to its good properties. Globally, 54 million tons of steel consume 3 million tons of zinc every year (Mudd et al., 2017; Abkhoshk et al., 2014). Unfortunately, with the continuous exploitation and utilization of zinc resources, the easily enriched zinc-sulfide ore has been gradually exhausted (Shi et al., 2012). Therefore, zinc-oxide ore with low grades and separation difficulty has become a research object of increasing experts and scholars (Yang et al., 2019).

As the main zinc-oxide ores, smithsonite is difficult to recover by methods using sulfide minerals due to its naturally strong hydrophilicity (Luo et al., 2020). Nowadays, several flotation separation methods, such as sulfidation flotation, fatty acid flotation, chelation flotation, flocculation flotation, and other technological methods, were established for zinc-oxide ores. Fatty acid collectors show poor selectivity in the flotation of smithsonite, especially when the ore contains gangue, such as calcite or dolomite (Bai et al., 2020). Due to its high cost and lack of long chain hydrocarbons, chelating trap has poor hydrophobicity. At present, there is no report on large-scale industrial applications. (Ejtemaei et al., 2014). Similarly, flocculation flotation is still in laboratory research stage for its non-ideal results (Sadowski and Polowczyk, 2004).

As the main separation method of oxide ore, sulfidation flotation refers to changing the surface properties of oxide ore minerals by using sulfidation and then recovering it via a collector. In the

process of sulfidation-xanthate flotation, the sulfidation agent hydrolyzes to produce  $S^{2-}$  or  $HS^-$ , which chemically interacts with the Zn ions exposed on the mineral surface to generate ZnS. After sulfidation, the surface properties of the mineral are similar to those of the natural zinc-sulfide minerals (Luo et al., 2019; Bai et al., 2020). The thin films increase the  $Zn^{2+}$  metal sites on the surface of smithsonite, thereby enhancing the adsorption of  $ROSS^-$  from xanthate and enabling the mineral to float (Ejtemaei et al., 2014). Sulfidation is generally an important prerequisite to realize efficient flotation in practice. The type of sulfurizing agent is vital for the sulfidation effect in flotation (Zuo et al., 2020). At present, sodium sulfide is the cheapest, effective and most widely used agent.

However, compared with that of other metal oxide minerals, such as malachite, the surface sulfidation of smithsonite by using sodium sulfide alone is a vastly difficult problem (Liu et al., 2019). In particular, long-term production practice shows that the dosage of sodium sulfide is strict (Cao et al., 2020). Once the content of  $HS^-$  in the pulp becomes excessive, it has an intense depression effect not only on sulfide ores but also on oxide mineral particles with sulfurized surface (Cao and Peng, 2018). A large number of studies have found that the sulfide film formed after long-time stirring is easy to fall off, which greatly reduces the sulfidation efficiency and affects the flotation behavior of minerals (Zhao et al., 2018). In addition, hydrogen sulfide gas was often produced when sodium sulfide was used, which seriously threatens the safety of workers and pollutes the environment (Yin et al., 2010). Critically, to improve the reactivity of sodium sulfide on the smithsonite surface, heating the pulp in production is necessary (Lan et al., 2020). The hydrothermal sulfidation-warm water flotation process was used in some concentrators to recover zinc-oxide minerals (Li et al., 2019). These processes have serious problems, such as high energy consumption and complex operation. All of the above are incompatible with the development trend of building green mines. Therefore, high-efficiency sulfidation agents of smithsonite have become a research hotspot.

From the perspective of structural chemistry, 1,3,5-Triazinane-2,4,6-trithione (TMT) hydrolysis could produce more  $S^{2-}$  sites complexed with metal ions than sodium sulfide hydrolysis. Fig. 1 shows the TMT molecular structure and dissolution process. TMT is widely used in industrial wastewater treatment due to its strong complexing ability with metal ions (Bailey et al., 2001). It does not produce hydrogen sulfide gas in the process; thus, it is free of pollution, in small dosage, with excellent effect, and is environmental friendly (Yazici et al., 2020). Furthermore, the agent may be adsorbed on the smithsonite surface in the form of tri-zinc complex precipitation, which provides more adsorption sites for collectors. Therefore, TMT may achieve a better sulfidation effect than sodium sulfide. The sulfidation effect of TMT and sodium sulfide in smithsonite was compared via conventional micro-flotation tests to verify this assumption. By the way, sulfidation mechanism of TMT was further studied using various analyses, including contact angle measurements, FTIR, Zeta potential analysis, ICP spectral detection, and solution chemical calculation. Finally, an agent action model was drawn for further illustration.

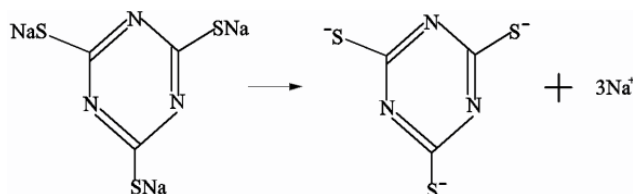


Fig. 1. TMT dissolution process

## 2. Materials and methods

### 2.1. Samples and agents

Smithsonite used for all experiments came from Yunnan Province, China. The ore with grain size  $<10$  mm was selected crushing by three agate grinders. Dry screen selected samples with grain size  $-74 +30$   $\mu\text{m}$  for micro-flotation tests and ICP spectrometer measurements. Moreover, the particle size  $>10$  mm was used for contact detection and size  $<5$   $\mu\text{m}$  for XRD, FT-IR and Zeta potential measurements. The purity of samples were analyzed via a chemical method and X-ray diffraction analysis (XRD).

Compared with references (Liu et al., 2021; Zeng et al., 2020), Fig. 2 indicated the high purity of smithsonite used in the experiment.

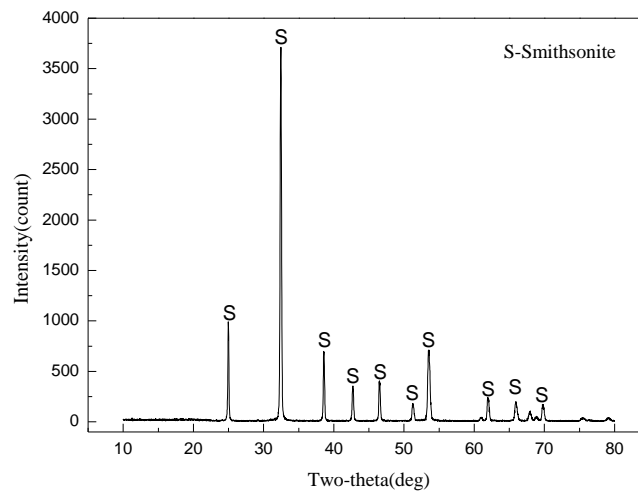


Fig. 2. XRD of smithsonite samples

All the agents used in the experiment were analytical grades. Hydrochloric acid (HCl) and sodium hydroxide (NaOH) were used to adjust the pH of pulp. Sodium sulfide ( $\text{Na}_2\text{S} \cdot 9\text{H}_2\text{O}$ ) was used as sulfidization. The foregoing was obtained from Aladdin Reagent Co. Ltd. (Shanghai, China). The agent of TMT was purchased from Guangdong Wengjiang Chemical Reagent Co. Ltd. (Guangdong, China). The industrial-grade sodium n-butyl xanthate (SBX) was used as collector. The solvent used in the experiment was deionized water.

## 2.2. Micro-flotation tests

The XFG<sub>115</sub> flotation machine with 40 mL flotation cell (Jilin Exploration Machinery Factory) was used in micro-flotation. The stirring speed was 1980 r/min. 2 g of pure smithsonite and 35 ml deionized water were added to the flotation cell. By the way, the pH was regulated by HCl or NaOH (0.1 mol/L) solution with 3 min stirring.  $\text{Na}_2\text{S}$ /TMT solution was subsequently added with a specific concentration and stirred for 5 min. Adding SBX solution and stirring for 3 min. Finally, the flotation was conducted for 4 min. The concentrates and tailing were collected respectively, recovery was calculated from the dry weights of them.

## 2.3. Contact angle measurement

The contact angle was measured using a KRUSS contact angle measuring instrument (DSA100, Germany). The pure mineral of smithsonite with grain size  $>10 \mu\text{m}$  was polished with 7  $\mu\text{m}$ , 5 $\mu\text{m}$ , 3 $\mu\text{m}$  sandpaper, and washed repeatedly with deionized water. Before measurement, samples were treated with different concentration of agents in a beaker, and dried at 25°C in vacuum oven for contact angle measurement. The polishing surface of the sample was placed upward on the measuring table, 4  $\mu\text{L}$  droplet of deionized water was deposited onto the polished face, and the contact angle was simultaneously measured. GBX software was used to calculate the three-phase interface angle. Each point was measured five times, and the average value was acquired.

## 2.4. FT-IR spectroscopy measurements

The FT-IR spectra was obtained using an AVATAR360 infrared spectrometer to characterize the interaction between the agent and minerals. Besides, the wavenumbers of spectrum tested were 400-4000  $\text{cm}^{-1}$ , each spectrum scanned 100 times and resolution was 4  $\text{cm}^{-1}$ . The background peaks of KBr were removed prior to the infrared study, and 1.0 mg of sample before or after treatment was then uniformly mixed with 100 mg of KBr particles. To prepare the samples for FT-IR analysis, the suspension was prepared by adding 2 g pure minerals and 35 ml deionized water in a beaker, and the

suspension was adjusted to pH~6.5 with HCl and NaOH solution.  $5 \times 10^{-5}$  mol/L Na<sub>2</sub>S/TMT solution was added and stirred for 5 min. Then  $5 \times 10^{-4}$  mol/L SBX solution was subsequently added and stirred for 10 min. Finally, the solution was filtered and washed repeatedly with deionized water 3 times. The precipitate dried at 45°C in vacuum oven for FT-IR spectroscopy measurements.

## 2.5. Zeta Potential measurements

Zeta potential measurement of smithsonite was conducted using a ZetaProbe Zeta Potential Analyzer (Colloidal Dynamics LLC, USA). Before measurements, buffer solution and KSiW liquid were used to correct the pH electrode and ESA electrode respectively, then the standard KCl solution was used as a conductivity calibration solution. Firstly, the 0.1g samples and 200 ml deionized water were added in cell cup and stirred for 5 min. The desired pH was adjusted by 0.1mol/L HCl or NaOH solutions, then the  $5 \times 10^{-5}$  mol/L Na<sub>2</sub>S/TMT was added. The stirring speed of the cell cup was 150 r/min. Finally, the zeta potential was measured by ESA electrode in the cell cup. For each measurement, the average value was obtained from 5 times tests.

## 2.6. ICP spectral detection and solution chemical calculation

The content of the corresponding elements in the solution can be determined according to the intensity of the characteristic spectral line (quantitative analysis). Owing to the smithsonite being a semi-soluble mineral, the flotation would be affected by the dissolved Zn<sup>2+</sup> and CO<sub>3</sub><sup>2-</sup> in the slurry. It is necessary to determine whether the sulfidation agent reacts with the ions in the solution.

Before ICP spectrum detection, 2g samples and 35ml deionized water were added in the flotation cell. The slurry pH was adjusted at 6.5 by HCl and NaOH. After stirring for 5 min, the sulfidation agent ( $5 \times 10^{-5}$  mol/L) was added and continuously stirred for 5 min. The supernatant of slurry in the absence and presence of sulfidation agent was taken for ICP spectrum detection.

The solution chemistry of smithsonite (ZnCO<sub>3</sub>), sodium sulfide (Na<sub>2</sub>S) and TMT were calculated respectively, and the sulfidation mechanism was analyzed.

## 3. Results and discussion

### 3.1. Microflotation tests

#### 3.1.1. Effect of pH on the flotation behavior of smithsonite in the absence and presence of sulfidation agent

As a kind of carbonate mineral, smithsonite will dissolve in pulp and produce a large amount of Zn<sup>2+</sup> and CO<sub>3</sub><sup>2-</sup>. With the change of acid-base environment, the original ion balance of pulp is broken, which has a great impact on the flotation behavior of minerals (Zhou et al., 2021). Fig. 3 shows the effect of pH on the flotation behavior of smithsonite in the absence and presence of sulfidation agent. In the absence of sulfidation, the floatability of smithsonite was poor when SBX was used as collector, with the highest recovery rate being only 44.75%. The sulfide film could be formed on the surface of the smithsonite after sodium sulfide treatment, thus enhancing the adsorption of butyl xanthate. However, with the addition of sodium sulfide, the effect was not obvious, and the recovery rate was increased only up to 55.35%. In comparison, 74.6% recovery rate was obtained after TMT treatment, significantly higher than that in sodium sulfide. By the way, with the increase of pulp alkalinity, the recovery rate gradually decreases. This is because the ion produced by the hydrolysis of smithsonite in alkaline environment interacts with the reagent, which greatly reduces the reagent adsorbed on the mineral surface (Zeng et al., 2020).

#### 3.1.2. Effect of sulfidation agent concentration on the flotation behavior of smithsonite

As the key of sulfurized flotation of oxide ore, the dosage of sulfidation plays an important role in the flotation recovery of oxide ore (Zeng et al., 2020). However, with the increase of the amount of most sulfidation, the flotation of oxide ore will be inhibited to a certain extent. Because most of the agents act as sulfidation of oxidized ore, they are also inhibitors of sulfide ore (Cui et al., 2020). Fig. 4 shows the effect of sulfidation agent concentration on the flotation behavior of smithsonite at pH 6.5.

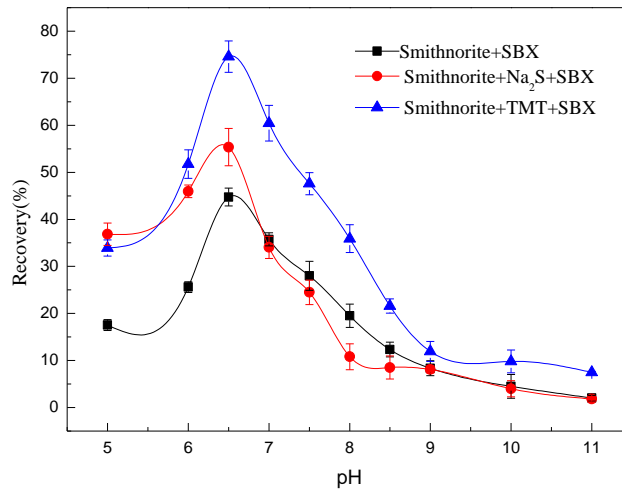


Fig. 3 . the recovery of smithsonite in the absence and presence of sulfidation agent at different pH value (Na<sub>2</sub>S/TMT:  $1 \times 10^{-4}$  mol/L, SBX:  $5 \times 10^{-4}$  mol/L)

Obviously, 80.5% recovery shows the effect of sulfidation agent concentration on the flotation behavior of smithsonite at pH 6.5. Obviously, 80.5% recovery rate was obtained after TMT treatment at the concentration of  $5 \times 10^{-5}$  mol/L, while the maximum recovery was 59.4% after sodium sulfide treatment under the same condition. The sulfidation effect of TMT was significantly better than that of sodium sulfide. However, with the increase in the dosage of sulfidation, the recovery rate decreased gradually. Thus, the dosage of sulfidation has considerable influence on the recovery.

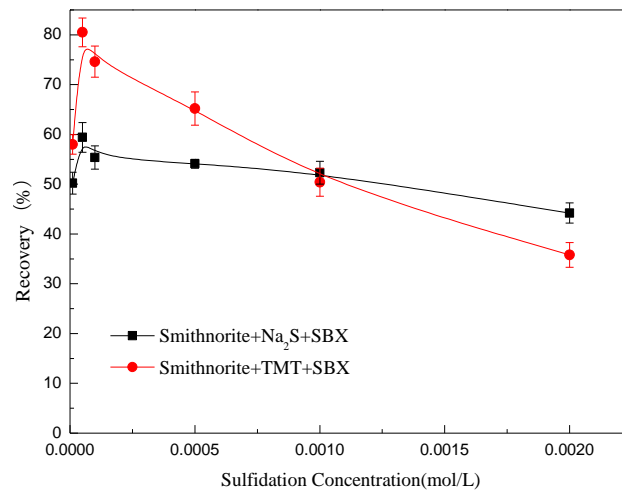


Fig. 4. Recovery of smithsonite with different concentrations of sulfidation agent at pH 6.5 (SBX:  $5 \times 10^{-4}$  mol/L)

### 3.2. Contact angle measurement

The hydrophobicity of mineral particles surface could be indirectly indicated by the change in the contact angle before and after treatment (Potapova et al., 2012). Fig. 5 shows the contact angle value and morphology of the smithsonite surface with the reaction of different reagents. The contact angle of fresh smithsonite was  $32.44^\circ$ , which showed strong hydrophilicity and poor floatability (Feng et al., 2019). However, with the addition of sodium sulfide, the contact angle increased from  $32.44^\circ$  to  $50.2^\circ$ . This change may be attributed to the formation of ZnS film on the smithsonite surface, and this formation increased the surface hydrophobicity. Besides, the contact angle further increased to  $57.78^\circ$  after TMT treatment.

After the reaction with butyl xanthate, the contact angle of smithsonite increased obviously, and the maximum contact angle of  $89.58^\circ$  was obtained when using TMT as sulfidation agent. The contact angle measurement further proved that the sulfidation effect of TMT was significantly better than that

of sodium sulfide, and it enhanced the adsorption of butyl xanthate, thereby increasing the surface hydrophobicity of smithsonite and improving the floatability.

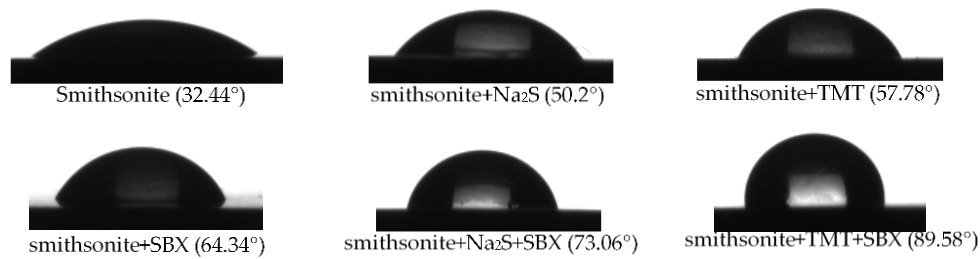


Fig. 5. Contact angle of smithsonite with or without agent treatment

### 3.3. FT-IR spectroscopy measurements

FT-IR was performed to better understand the action mechanism of smithsonite with TMT and contrast with sodium sulfide. The FT-IR spectra of agent and smithsonite treated with agent were shown in Fig. 6, Fig. 7 and Fig. 8, respectively.

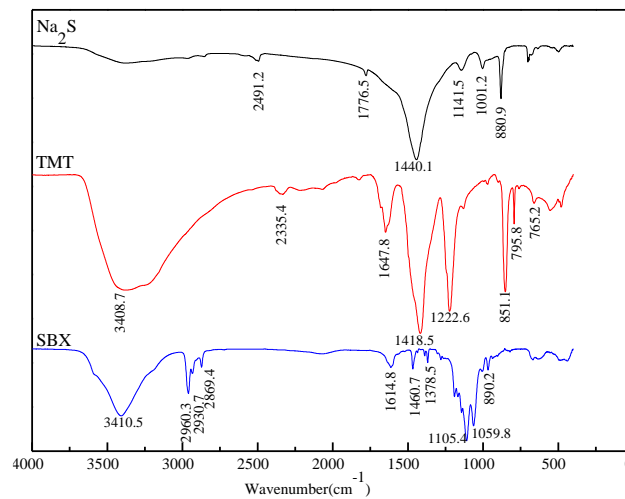


Fig. 6. IF-IR spectra of the agent

As shown in Fig. 6, the absorption peak of TMT at 3408.7 cm<sup>-1</sup> was attributed to -OH stretching vibration, which may be caused by the adsorption of water vapor from the air (Wang et al., 2020). In the spectra, the S-H stretching vibration was observed at 2335.4 cm<sup>-1</sup> (Ceconi et al., 2002). The bands at 1647.8 and 1418.5 cm<sup>-1</sup> could be attributed to the C=N stretching vibration on the triazine ring. According to previous studies, the bands at 1222.6, 851.1, 795.8, and 765.2 cm<sup>-1</sup> were associated with the C-S stretching vibration (Yazici et al., 2020). In the infrared spectrum of butyl xanthate, the bands at 3410.5 and 1614.8 cm<sup>-1</sup> could be attributed to the O-H stretching vibration, which may be caused by the residual moisture in potassium bromide tablets (Zhu et al., 2018). In addition, the peaks at 2960.3 and 2869.4 cm<sup>-1</sup> of butyl xanthate could be attributed to the symmetric and asymmetric stretching vibration of -CH<sub>3</sub> groups, respectively (Wang et al., 2019). The band at 2930.7 cm<sup>-1</sup> could be attributed to the -CH<sub>2</sub> groups. The symmetric and asymmetric deformation vibration of the -CH<sub>3</sub> groups appeared at 1460.7 and 1378.5 cm<sup>-1</sup> (Bai et al., 2018). The stretching vibrations of C-O-C and C=S were observed at 1105.4 and 1059.8 cm<sup>-1</sup>, respectively. Furthermore, in the spectra of sodium sulfide, the band at 890.2 cm<sup>-1</sup> was assigned to C-S asymmetric stretching vibration (Zhu et al., 2018), the peak at 1440.1 cm<sup>-1</sup> was attributed to the bending vibration of O-H, and the band at 1141.5 cm<sup>-1</sup> was attributed to the S-H stretching vibration.

Fig. 7 shows the infrared spectral of smithsonite in the presence and absence of sulfidation agents. According to previous studies (Frost et al., 2008), the band at 1423.4 cm<sup>-1</sup> could be attributed to an asymmetric stretching vibration of the -CO<sub>3</sub> groups. The peak at 868.3 cm<sup>-1</sup> in the spectra was

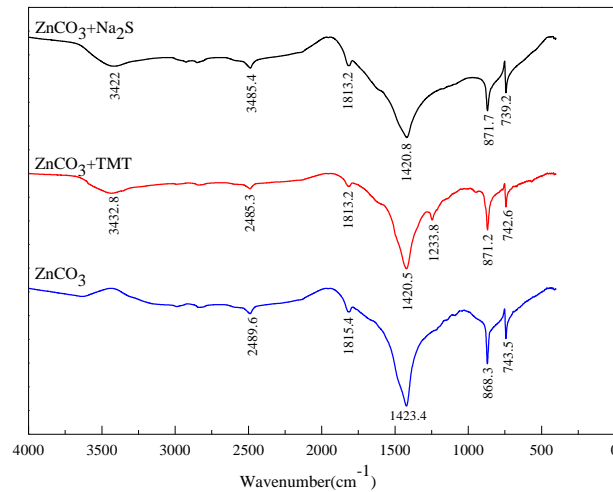


Fig. 7. FT-IR spectra of pH~6.5, the smithsonite before and after sulfidation

associated with the out-of-plane bending vibration of  $-\text{CO}_3$  groups, and the band at  $743.5 \text{ cm}^{-1}$  was assigned to the in-plane bending vibration of the  $-\text{CO}_3$  groups. All of them were infrared characteristic peaks of smithsonite (Frost et al., 2008). After TMT treatment, the new peak of C-S stretching vibration was observed at  $1233.8 \text{ cm}^{-1}$ , and the wavenumbers were shifted to  $11 \text{ cm}^{-1}$  compared with that of TMT. This finding indicated that TMT was chemically adsorbed on the smithsonite. In comparison, the infrared spectra of smithsonite before and after reaction with  $\text{Na}_2\text{S}$  were basically the same, no new absorption peaks were observed. However, the peak of the  $-\text{CO}_3$  groups was obviously weakened. The reason is probably because the solubility coefficient of  $\text{ZnS}$  and  $\text{ZnCO}_3$  were  $1.6 \times 10^{-24}$  and  $1.4 \times 10^{-11}$ , respectively, indicating that the solubility product of  $\text{ZnS}$  was significantly smaller than that of  $\text{ZnCO}_3$ . In addition, the  $\text{ZnS}$  and  $\text{ZnCO}_3$  bands are very similar. The  $\text{ZnCO}_3$  species after sulfidization -disappears and completely forms the  $\text{ZnS}$  coating in the case of very high  $\text{Na}_2\text{S}$  concentrations in the form of one monolayer or a little more (Marabini and Rinelli, 1986; Malghan S G., 1986). Therefore, the  $\text{S}^{2-}$  in sodium sulfide replaced the  $\text{CO}_3^{2-}$  groups on the smithsonite surface to form  $\text{ZnS}$  films, which reduced the solubility of mineral surface and reduced the adsorption peak of the  $-\text{CO}_3$  groups (Liu et al., 2016).

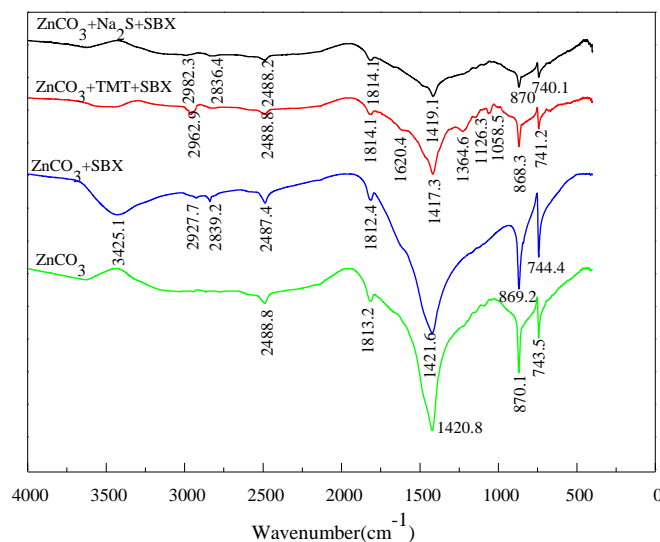


Fig. 8. IF-IR spectra of pH~6.5, the smithsonite before and after treatment

Fig. 8 shows that SBX could be adsorbed on the smithsonite. After SBX treatment, the asymmetric stretching vibration of the  $-\text{CH}_2$  and  $-\text{CH}_3$  groups appeared at  $2927$  and  $2839 \text{ cm}^{-1}$ . In comparison, before and after  $\text{Na}_2\text{S}$  treatment, the SBX characteristic peaks barely changed, which indicated the

weak effect of  $\text{Na}_2\text{S}$  on smithsonite. By contrast, after TMT treatment, the strength of the  $-\text{CH}_2$  group asymmetric stretching vibration was significantly enhanced. Furthermore, the asymmetric deformation vibration peak of the  $-\text{CH}_3$  groups, the C-O-C vibration peak, and the C=S telescopic vibration peak obviously appeared at  $1364.6$ ,  $1126.3$ , and  $1058.5 \text{ cm}^{-1}$ , respectively, indicating that more butyl xanthate was adsorbed on the mineral surface.

The FT-IR spectroscopy measurements results showed that TMT could be chemically adsorbed more strongly on the smithsonite surface, and it significantly enhanced the adsorption of SBX compared with  $\text{Na}_2\text{S}$ .

### 3.4. Zeta potential measurements

When adsorption occurs in the Stern layer, the Zeta potential of minerals usually changes. Thus, zeta potential measurements were performed to explain the adsorption strength difference in  $\text{Na}_2\text{S}$  and TMT. Fig. 9 shows the zeta potential of smithsonite as a function of pH in the absence and presence of sulfidation.

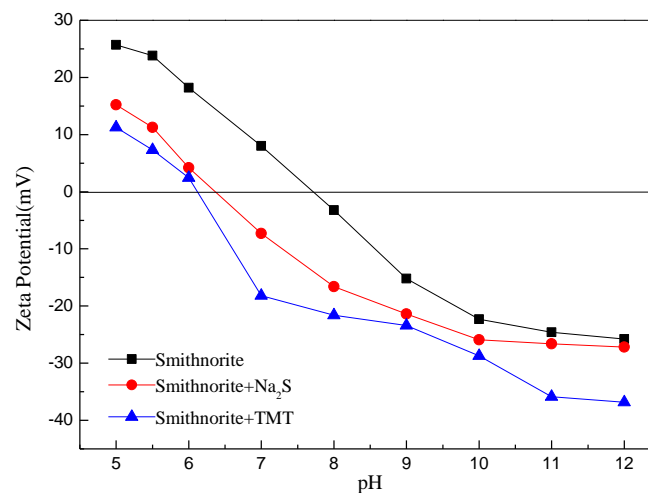


Fig. 9. Zeta potential of smithsonite before and after sulfidation agent treatment

The isoelectric point of smithsonite was pH 7.8, which was similar to that reported in Ref (Shi et al., 2012). The zeta potential of smithsonite was negative in a wide range of pH, and the negative of potential increased sharply with the increase in pH. Given that smithsonite is a semi-soluble mineral, non-stoichiometric dissolution occurs in the solution to produce surface charges, leading to the hydrolysis of ions released into the solution (Wu et al., 2017). The adsorption of free anions and cations in pulp on mineral surface results in the change of mineral surface potential. Therefore, when  $\text{pH} < 7.8$ , the re-adsorption ions are mainly  $\text{Zn}^{2+}$ ,  $\text{ZnOH}^+$ , and  $\text{ZnHCO}_3^+$ , indicating that the electrical properties of the mineral surface is positive (Shi et al., 2013). With the decrease in pH, several  $\text{H}^+$  ions in the solution lead to the decrease in cation dissolved in the mineral. Thus, the surface electrical properties decreased gradually. On the contrary, with  $\text{pH} > 7.8$ , the re-adsorption ions were dominated by  $\text{CO}_3^{2-}$ ,  $\text{Zn}(\text{OH})_3^-$ , and  $\text{Zn}(\text{OH})_4^{2-}$ , and the surface electrical properties of mineral is negative (Ju et al., 2005). With the increase of pulp alkalinity, the anions produced by the hydrolysis of smithsonite increase gradually. Therefore, the surface electrical properties are gradually improved.

The zeta potential of smithsonite decreased in the presence of sodium sulfide as a function of pH, suggesting that  $\text{HS}^-$  or  $\text{S}_2^-$  were adsorbed on the smithsonite surface and made the smithsonite surface charge more negative (Bai et al., 2020). With TMT treatment, the isoelectric point (IEP) of smithsonite appeared around pH 6. Due to the TMT hydrolysis occurring at pH 6,  $\text{TMT}^{3-}$  was absorbed on the mineral surface, resulting in forward IEP. The change of zeta potential before and after the treatment of TMT proved that TMT could be chemically adsorbed on the surface of smithsonite. The combination of micro-flotation test and FTIR spectroscopy measurements showed that the chemisorption of TMT was stronger than that of sodium sulfide. Therefore, the sulfidation of TMT was more effective, which is beneficial for the adsorption of collectors on minerals.



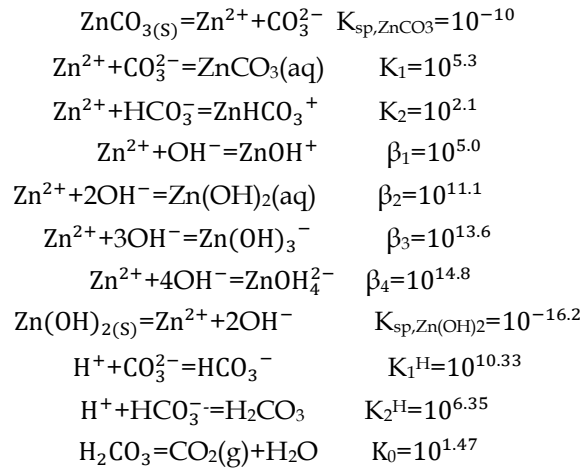
### 3.5. ICP spectral detection and solution chemical calculation

Solution chemical calculations play a major role in studying the behavior of flotation systems. By applying solution chemical calculations to a salt-type mineral and inorganic depressant flotation system, the critical depression pH and depressant concentration were predicted precisely (Hu et al., 2003). Table 1 shows the change in the  $Zn^{2+}$  content of smithsonite pulp before and after sulfidation. Before sulfidation agent treatment, 146.51 mg/L of  $Zn^{2+}$  was dissolved in the smithsonite pulp at pH 6.5. With sodium sulfide treatment, the content of  $Zn^{2+}$  decreased to 109.3 mg/L, indicating that  $Zn^{2+}$  could be reabsorbed on the S sites after the  $HS^-$  absorption on the smithsonite surface. However, the re-adsorption of  $Zn^{2+}$  was not obvious, probably because of the weak adsorption of  $HS^-$  on the minerals, as indicated by FTIR analysis and zeta potential measurements, and the less S sites provided to the  $Zn^{2+}$  in the solution. After TMT treatment, the content of  $Zn^{2+}$  in the pulp sharply decreased to 22.09 mg/L. Thus,  $Zn^{2+}$  was intensively re-adsorbed on the smithsonite surface. Compared with the molecular structure of  $Na_2S$  and TMT, the increased S sites of TMT for the adsorption of  $Zn^{2+}$  are the main cause (Li et al., 2017). When one S atom in the TMT molecule was adsorbed on the mineral surface, the other two S atoms could combine with the  $Zn^{2+}$  in the pulp (Mostofa et al., 2021). Therefore, the content of  $Zn^{2+}$  in the pulp was much lower, and the adsorption strength of SBX was enhanced significantly. In order to verify this analysis, the solution chemistry calculation was carried out and the vulcanization mechanism of the agent was discussed.

Table 1. ICP detection the concentration of  $Zn^{2+}$  in smithsonite solution before and after treatment

	Smithsonite without treatment	TMT treatment	Na <sub>2</sub> S treatment
The concentration of $Zn^{2+}$	146.5mg/L	20.09mg/L	109.3mg/L

The following equilibrium exists in the smithsonite saturated solution (Shi et al., 2013):



In the atmosphere,  $PCO_2 = 10^{-3.5} \text{ atm}$ ,  $[H_2CO_3] = PCO_2 / K_0 = 10^{-4.97}$ , and  $\lg[H_2CO_3] = -4.97$ . Concentrations of the remaining components were pH as follows:

$$\begin{aligned} \lg[HCO_3^-] &= -11.32 + \text{pH} \\ \lg[CO_3^{2-}] &= -21.65 + 2\text{pH} \\ \lg[ZnCO_3(aq)] &= -4.7 \\ \lg[Zn^{2+}] &= -11.65 - 2\text{pH} \\ \lg[ZnOH^+] &= 2.65 - \text{pH} \\ \lg[Zn(OH)_2(aq)] &= -5.25 \\ \lg[Zn(OH)_3^-] &= -11.75 + \text{pH} \\ \lg[ZnOH_4^{2-}] &= -29.55 + 2\text{pH} \\ \lg[ZnHCO_3^+] &= 2.43 - \text{pH} \end{aligned}$$

According to the above formula, the logarithmic diagram of the concentration of the dissolved components of the smithsonite is drawn (Pokrovsky and Schott, 2002), Fig. 10.

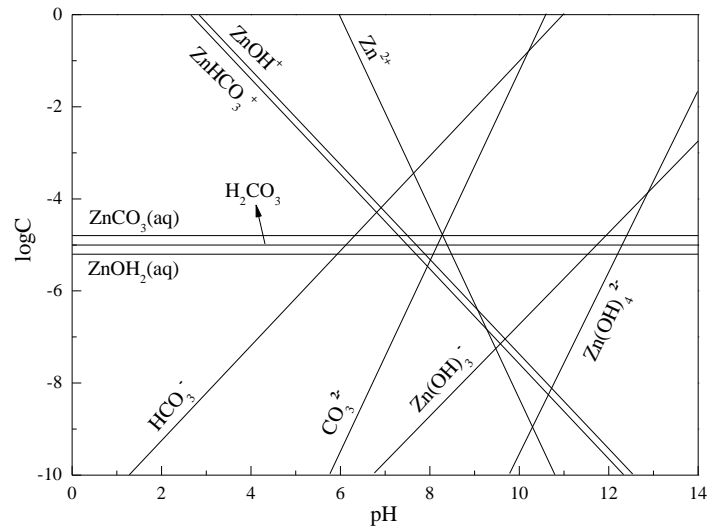
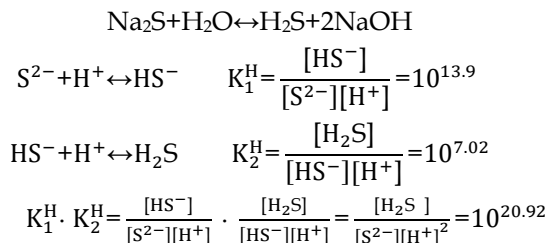


Fig. 10. Effect of pH on soluble component distribution of smithsonite

From Fig. 10, it can be seen that the smithsonite produced  $Zn^{2+}$ ,  $ZnOH^+$ ,  $HCO_3^-$ ,  $Zn(OH)_3^-$ ,  $Zn(OH)_4^{2-}$ ,  $CO_3^{2-}$ ,  $ZnHCO_3^+$  and  $H_2CO_3$ ,  $Zn(OH)_2(aq)$ ,  $ZnCO_3(aq)$  molecules after dissolving in deionized water (Shi et al., 2013). With the increasing pH of the solution system, the concentration of  $Zn^{2+}$ ,  $ZnOH^+$ ,  $ZnHCO_3^+$  in the solution decreases, concentrations of  $HCO_3^-$ ,  $Zn(OH)_3^-$ ,  $Zn(OH)_4^{2-}$ ,  $CO_3^{2-}$  are increasing. Fig. 10 shows that the ions dissociated in the solution are mainly  $Zn^{2+}$  at pH 6.5, which is consistent with ICP test results.

Sodium sulfide first hydrolyzes in water, then dissociates (Lebedev et al., 2020):



Total concentration of solution:

$$[S] = [S^{2-}] + [HS^-] + [H_2S]$$

Distribution coefficients of each component of the solution:

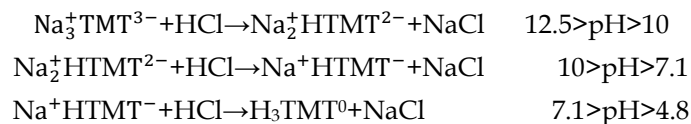
$$\phi_{[S^{2-}]} = \frac{[S^{2-}]}{[S^{2-}] + [HS^-] + [H_2S]} = \frac{1}{1 + K_1^H \cdot [H^+] + K_1^H \cdot K_2^H [H^+]^2}$$

$$\phi_{[HS^-]} = \frac{[HS^-]}{[S^{2-}] + [HS^-] + [H_2S]} = \frac{K_1^H \cdot [H^+]}{1 + K_1^H \cdot [H^+] + K_1^H \cdot K_2^H [H^+]^2}$$

$$\phi_{[H_2S]} = \frac{[H_2S]}{[S^{2-}] + [HS^-] + [H_2S]} = \frac{K_1^H \cdot K_2^H [H^+]^2}{1 + K_1^H \cdot [H^+] + K_1^H \cdot K_2^H [H^+]^2}$$

On the basis of the above formula, the  $\phi$ -pH diagram of sodium sulfide solution was showed in Fig. 11. It is shown there that at  $7 > pH > 4$ , the solution is dominated by  $H_2S$  and  $11 > pH > 7$  by  $HS^-$  (Lebedev et al., 2020). At pH 6.5, a small amount of  $HS^-$  and most of the  $H_2S$  are produced.

The dissolution of 1,3,5-triazinane-2,4,6-trithione (TMT) in hydrochloric acid is as follows (Bailey et al., 2001):



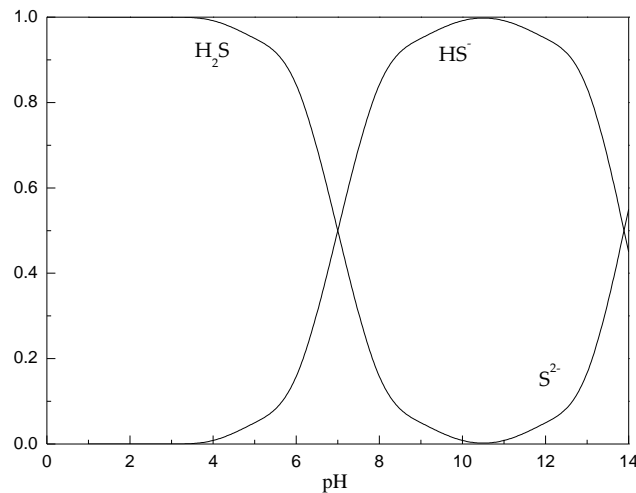
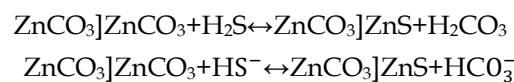


Fig. 11. Relationship between distribution coefficient and pH of components containing S in sodium sulfide solution

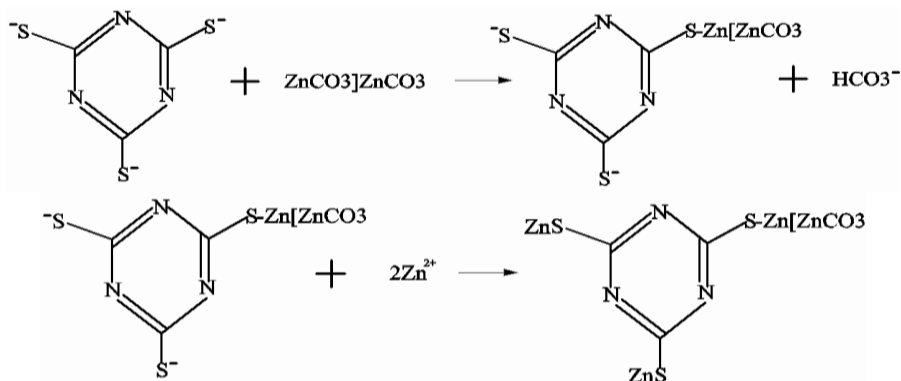
The above formula shows that when pH is about 6.5, the TMT solution is mainly  $H_3TMT$ .

At pH 6.5,  $Zn^{2+}$  and most of the  $H_2S$  and a few of the  $HS^-$  were the main components in solution of pulp (Mostofa et al., 2021). The following reactions occur on the surface of the smithsonite:



The analysis shows that a layer of ZnS film is formed on the surface of smithsonite after sodium sulfide treatment. However, due to less unstable  $H_2S$  and  $HS^-$ , the newly formed sulfide film is thin and unstable, and the improvement of the floatability of smithsonite is very limited (Xie et al., 2020).

Using TMT as sulfidation agent, at pH 6.5, the  $Zn^{2+}$  and  $H_3TMT$  are the main components in solution of pulp, and the reaction occurs on the surface of the mineral as follows (Bailey et al., 2001):



The sulfidation agent TMT can provide more adsorption sites for the adsorption of butyl xanthate. Fig. 12 shows the sulfidation and xanthate adsorption models on the surface of smithsonite particles.

#### 4. Conclusions

Using TMT as sulfidation agent could improve the flotation recovery of smithsonite. The results of micro-flotation tests showed that the sulfidation effect of TMT was better than that of sodium sulfide. According to the contact angle test, TMT could considerably increase the surface hydrophobicity of the smithsonite, and the hydrophobic effect was more obvious than that in sodium sulfide. The results of FTIR spectroscopy, Zeta potential test, ICP test, and solution chemical calculation showed that TMT was chemically adsorbed on the smithsonite surface. In addition, the adsorption strength of TMT was significantly higher than that of sodium sulfide. Increased S sites could be provided for the adsorption of  $Zn^{2+}$  dissolved in the smithsonite pulp due to the special molecular structure of TMT. Thus,  $Zn^{2+}$  was re-adsorbed on the smithsonite surface intensively, and more sites were formed, which could

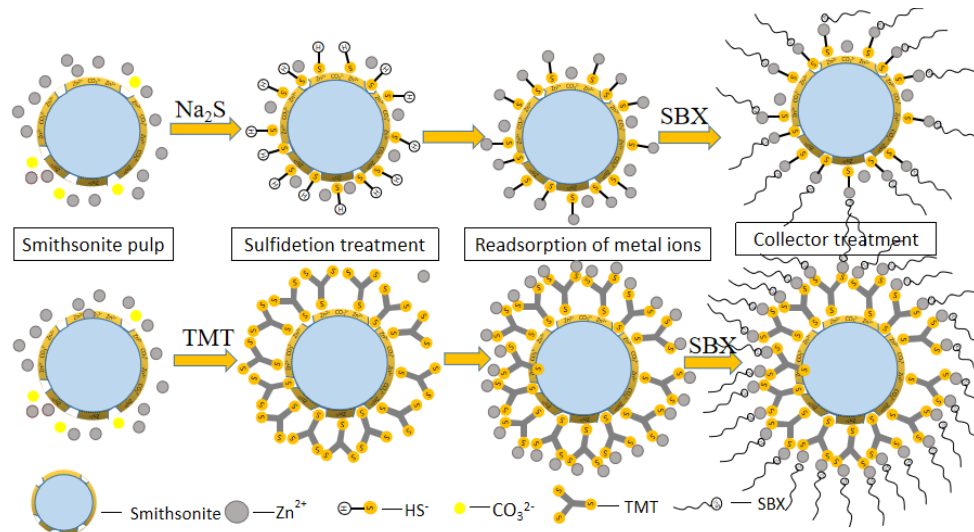


Fig. 12. Model of action of mineral particles and agents

significantly enhance the adsorption of SBX. Finally, the floatability of smithsonite was improved, more butyl xanthate was absorbed on the smithsonite particle surface, and enhanced flotation of the smithsonite was realized. TMT generally has a better application prospect than sodium sulfide in zinc-oxide ore flotation.

### Acknowledgments

This work was supported by The Major scientific and technological projects of Qinghai Province (grant no. 2018-GX-A7), and National Science and technology award reserve project cultivation plan project (grant no.20192AEI91003).

### References

- ABKHOSHK, E., JORJANI, E., AL-HARAHSEH, M, S., RASHCHI, F., NAAZERI, M., 2014. *Review of the hydrometallurgical processing of non-sulfide zinc ores*. Hydrometallurgy. 149, 153-167.
- BAI, S., LI, C., FU, X., LIU, J., WEN, S., 2018. *Characterization of zinc sulfide species on smithsonite surfaces during sulfidation processing: Effect of ammonia liquor*. J. Ind. Eng. Chem. 61, 19-27.
- BAI, S., YU, P., DING, Z., LI, C., XIAN, Y., WEN, S., 2020. *Ammonium chloride catalyze sulfidation mechanism of smithsonite surface: Visual MINTEQ models, ToF-SIMS and DFT studies*, Miner. Eng. 146, 106115.
- BAI, X., LIU, J., WEN, S., WANG, Y., 2020. *Utilization of local electrochemical impedance spectroscopy to study the attenuation law of the sulfide layer on the surface of smithsonite*. Powder Technol. 373, 754-757.
- BAI, X., LIU, J., WEN, S., WANG, Y., LIN, Y., 2020. *Effect of ammonium salt on the stability of surface sulfide layer of smithsonite and its flotation performance*. Appl. Surf. Sci. 514, 145851.
- BAILEY, J, R., JASONHATFIELD, M., HENKE, K, R., KREPPS, M, K., MORRIS, J, L., TOMOTIENO, T., SIMONETTI, K, D., WALL, E, A., ATWOOD, D, A., 2001. *Transition metal complexes of 2,4,6-trimercapto-1,3,5-triazine (TMT): potential precursors to nanoparticulate metal sulfides*. J. Organomet. Chem. 623, 185-190.
- CAO, Z., CHEN, X., PENG, Y., 2018. *The role of sodium sulfide in the flotation of pyrite depressed in chalcopyrite flotation*. Miner. Eng. 119, 93-98.
- CAO, Z., WANG, P., ZHANG, W., ZENG, X., CAO, Y., 2020. *Mechanism of sodium sulfide on flotation of cyanide-depressed pyrite*. T. Nonferr. Metal. SOC. 2, 484-491.
- CECCONI, F., GHILARDI, C, A., MIDOLLINI, S., ORLANDINI, A., 2002. *Organomercury derivatives of the 2,4,6-trimercaptotriazine(H3TMT). X-ray crystal structure of (HgMe)3(TMT)*. J. Organomet. Chem. 1, 101-104.
- CUI, W., CHEN, J., LIA, Y., CHEN, Y., ZHAO, C., 2020. *Interactions of xanthate molecule with different mineral surfaces: A comparative study of Fe, Pb and Zn sulfide and oxide minerals with coordination chemistry(Article)*. Miner. Eng. 159, 106565.

- EJTEMAEI, M., GHARABAGHI, M., IRANNAJAD, M., 2014. *A review of zinc oxide mineral beneficiation using flotation method*. Adv. Colloid Interface Sci. 206, 68-78.
- FENG, Q., WEN, S., BAI, X., CHANG, W., CUI, C., ZHAO, W., 2019. *Surface modification of smithsonite with ammonia to enhance the formation of sulfidization products and its response to flotation*. Miner. Eng. 137, 1-9.
- FROST, R. L., MARTENS, W. N., WAIN, D. L., HALES, M. C., 2008. *Infrared and infrared emission spectroscopy of the zinc carbonate mineral smithsonite*. Spectrochim. Acta. A. 70, 1120-1126.
- HU, Y., CHI, R., XU, Z., 2003. *Solution chemistry study of salt-type mineral flotation systems: role of inorganic dispersants*. Ind. Eng. Chem. Res. 42, 1641-1647.
- JU, S., TANG, M., YANG, S., LI, Y., 2005. *Dissolution kinetics of smithsonite ore in ammonium chloride solution*. Hydrometallurgy. 80, 67-74.
- LAN, Z., LAI, Z., ZHENG, Y., LU, J., PANG, J., NING, J., 2020. *Thermochemical modification for the surface of smithsonite with sulfur and its flotation response*. Miner. Eng. 150, 106271.
- LEBEDEV, M. V., SEROV, Y. M., LVOVA, T. V., ENDO, R., MASUDA, T., SEDOVA, L. V., 2020. *InP(1 0 0) surface passivation with aqueous sodium sulfide solution*. Appl. Surf. Sci. 533, 147484.
- LI, C., BAI, S., DING, Z., YU, P., WEN, S., 2019. *Visual MINTEQ model, ToF-SIMS, and XPS study of smithsonite surface sulfidation behavior: Zinc sulfide precipitation adsorption*. J. Taiwan. INST. Cheme. 96, 53-62.
- LI, Q., LI, S., WANG, K., ZHOU, Y., QUAN, Z., MENG, Y., MA, Y., ZOU, B., 2017. *Structural tuning and piezoluminescence phenomenon in trithiocyanuric acid(Article)*. J Phys Chem C. 121, 1870-1875.
- LIU, C., FENG, Q., ZHANG, G., MA, W., MENG, Q., CHEN, Y., 2016. *Effects of lead ions on the flotation of hemimorphite using sodium oleate*. Miner. Eng. 89, 163-167.
- LIU, C., SONG, S., LI, H., AI, G., 2019. *Sulfidization flotation performance of malachite in the presence of calcite*. Miner. Eng. 132, 293-296.
- LIU, C., WANG, X., YANG, S., REN, Z., LI, C., HU, Z., 2021. *Utilization of polyepoxysuccinic acid as a green depressant for the flotation separation of smithsonite from calcite*. Miner Eng. 168, 106933.
- LUO, B., LUI, Q., DENG, J., YU, L., LAI, H., SONG, C., LI, S., 2019. *Characterization of sulfide film on smithsonite surface during sulfidation processing and its response to flotation performance*. Powder Technol. 351, 144-152.
- LUO, Y., ZHANG, G., MAI, Q., LIU, H., LI, C., FENG, H., 2020. *Flotation separation of smithsonite from calcite using depressant sodium alginate and mixed cationic/anionic collectors*. Colloid. Surface. A. 586, 124227.
- MALGHAN, S. G., 1986. *Role of sodium sulfide in the flotation of oxidized copper, lead, and zinc ores*. Mining Metall Explor. 3, 158-163.
- MARABINI, A. M., RINELLI, G., 1986. *Flotation of lead-zinc oxide ores*. Advances in Mineral Processing, Proceedings of a Symposium Honoring Nathaniel Arbutnot, P Somasundaran, ed. 269-288.
- MOSTOFA, A., ZHENG, J., MAJUMDER, M., WEI, W., ZHOU, Y., WANG, S., ZHOU, Y., DENG, Z., 2021. *Interfacial properties of trithiocyanuric acid functionalized cellulose nanofibers for efficient recovery of gold ions from aqueous solution*. Cellulose. 28, 937-947.
- MOSTOFA, A., ZHENG, J., MAJUMDER, M., WEI, W., ZHOU, Y., WANG, S., ZHOU, Y., DENG, Z., 2021. *Interfacial properties of trithiocyanuric acid functionalized cellulose nanofibers for efficient recovery of gold ions from aqueous solution*. Cellulose. 28, 937-947.
- MUDD, G. M., JOWITT, S. M., WERNER, T. T., 2017. *The world's lead-zinc mineral resources: Scarcity, data, issues and opportunities*. Ore. Geol. Rev. 80, 1160-1190.
- POKROVSKY, O. S., SCHOTT, J., 2002. *Surface Chemistry and Dissolution Kinetics of Divalent Metal Carbonates*. Environ. Sci. Technol. 36, 326-432.
- POTAPOVA, E., YANG, X., WESTERSTRAND, M., GRAHN, M., HOLMGREN, A., HEDLUND, J., 2012. *Interfacial properties of natural magnetite particles compared with their synthetic analogue*. Miner. Eng. 36, 187-194.
- SADOWSKI, Z., POLOWCZYK, L., 2004. *Agglomerate flotation of fine oxide particles*. Int. J. Miner. Process. 74, 85-90.
- SHI, Q., FENG, Q., ZHANG, G., DENG, H., 2012. *Electrokinetic properties of smithsonite and its floatability with anionic collector*. Colloid. Surface. A. 410, 178-183.
- SHI, Q., FENG, Q., ZHANG, G., DENG, H., 2012. *Electrokinetic properties of smithsonite and its floatability with anionic collector*. Colloids Surf. A. 410, 178-183.
- SHI, Q., ZHANG, G., FENG, Q., DENG, H., 2013. *Effect of solution chemistry on the flotation system of smithsonite and calcite*. INT. J. Miner. Process. 119, 34-39.
- WANG, L., HU, G., SUN, W., KHOSO, S. A., LIU, R., ZHANG, X., 2019. *Selective flotation of smithsonite from dolomite by using novel mixed collector system*. T. Nonferr. Metal. SOC. 29, 1082-1089.

- WANG, Q., ZHENG, C., ZHAN, J., HE, F., YAO, Y., ZHANG, T., HE, C., 2020. *Insights into the adsorption of Pb(II) over trimercapto-s-triazine trisodium salt-modified lignin in a wide pH range*. Chem. Eng. J. A. 1, 100002.
- WU, D., MA, W., WEN, S., BAI, S., DENG, J., YIN, Q., 2017. *Contribution of ammonium ions to sulfidation-flotation of smithsonite*. J. Taiwan Inst Chem. E. 78, 20-26.
- XIE, H., SUN, R., WU, J., FENG, D., GAO, L., 2020. *A Case Study of Enhanced Sulfidization Flotation of Lead Oxide Ore: Influence of Depressants*. Minerals. 10, 95.
- YANG, Y., GUO, H., CHEN, L., LIU, X., GU, M., KE, X., 2019. *Regional analysis of the green development level differences in Chinese mineral resource-based cities*. Resources Policy. 61, 261-272.
- YAZICI, E. Y., AHLATCI, F., YILMAZ, E., CELEP, O., DEVECI, H., 2020. *Precipitation of zinc from cyanide leach solutions using Trimercapto-s-triazine (TMT)*. Hydrometallurgy. 191, 105206.
- YIN, W., ZHANG, L., XIE, F., 2010. *Flotation of Xinhua molybdenite using sodium sulfide as modifier*. rans. Nonferrous Met. Soc. China. 20, 702-706.
- ZENG, Y., LIU, J., LIU, J., DONG, W., HAO, J., WANG, Y., 2020. *Study on Sulfide Layer Attenuation Behavior of Smithsonite During Sulfidization Flotation*. Front Mater. 6.
- ZHAO, Q., LIU, W., WEI, D., WANG, W., CUI, B., LIU, W., 2018. *Effect of copper ions on the flotation separation of chalcopyrite and molybdenite using sodium sulfide as a depressant*. Miner. Eng. 115, 44-52.
- ZHOU, H., YANG, Z., ZHANG, Y., XIE, F., LUO, X., 2021. *Flotation separation of smithsonite from calcite by using flaxseed gum as depressant*. Miner. Eng. 167, 106904.
- ZHU, H., QIN, W., CHEN, C., CHAI, L., LI, L., LIU, S., ZHANG, T., 2018. *Selective flotation of smithsonite, quartz and calcite using alkyl diamine ether as collector*. T. Nonferr. Metal. SOC. 28, 163-168.
- ZUO, Q., YANG, J., SHI, Y., WU, D., 2020. *Activating hemimorphite using a sulfidation-flotation process with sodium sulfosalicylate as the complexing agent*. J. Mater. Res. Technol. 9, 10110-10120.